CVD grown Graphene Microfilms as a Promising Microscaled Solid Lubricant for the Lubrication of Silicon MEMS Devices

Muhammad Chhattal (chhattal@outlook.com)
Lanzhou Institute of Chemical Physics State Key Laboratory of Solid Lubrication
https://orcid.org/0000-0002-8804-2277
Abdul Ghaffar
UCAS: University of the Chinese Academy of Sciences
Fayaz Ali Dharejo
UCAS: University of the Chinese Academy of Sciences
Salamat Ali
Lanzhou University

Research Article

Keywords: MEMS Lubrication, Friction, Wear, Chemical Vapor Deposition, Graphene microfilms, PMMA transfer

Posted Date: April 1st, 2021

DOI: https://doi.org/10.21203/rs.3.rs-367495/v1

Abstract

Friction, wear, stiction, adhesion, and absence of suitable lubrication methods are important challenges, severely restricting and limiting the expeditious development of Microelectromechanical system (MEMS) technology. This paper aims to explore the potential of chemical vapor deposition (CVD) grown graphene microfilms for the lubrication of sliding silicon MEMS devices to reduce friction and wear problems. A novel silicon-based pin-on-disk friction-pair is designed to mimic sliding MEMS working conditions. Pure graphene-based microfilms are fabricated on the Cu substrate via a CVD method and transferred to the silicon substrate via the PMMA transfer method. To investigate microfilms' surface quality and morphology, microfilms are characterized via Raman spectroscopy, AFM, and SEM. For the tribological performance evaluation, different tribological tests were conducted using the microtribometer. Results show that microfilms remarkably reduced the friction coefficient and wear in the MEMS devices; however, microfilms' tribological performance depends on the roughness and the number of films on the specimen. This remarkable tribological performance suggests that graphene microfilms have the potential to increase the reliability and wear lifespan of MEMS devices. It is foreseeable that this lubrication method can be a step towards the expeditious industrial development of silicon MEMS devices.

1 Introduction

MEMS technology's expeditious growth has made significant contributions to human life by producing a tremendous number of MEMS devices such as ink-jet printers, digital micromirrors, accelerometers, and inertial sensors, but also brought many challenges. Friction, wear, stiction, and adhesion are imperious challenges, severely restricting silicon MEMS devices' development. Consequently, most commercial MEMS products do not have sliding contacts because MEMS devices with sliding contacts, such as micro gears, micro motors, micromirrors, have a short lifespan and are worn out easily prolonged running in operation [1]. The main reason for MEMS devices' failure is the substrate material silicon; the inherited properties of silicon, such as surface roughness, brittleness, and non-lubricious nature, make it vulnerable to wear, stiction, friction, and adhesion [2]. Therefore, the reduction of friction, adhesion, and wear is of great importance for MEMS devices' development and mass production. So far, to avoid or reduce friction and wear problems, tribologists have reported vapor phase lubrication, liquid lubrication, and coatings methods to improve MEMS device's lifetime and reliability of devices.

Asay, Dugger [3] had shown that Vapour Phase lubrication is satisfactory for small-scaled sliding systems because it confirms that the lubricant is uniformly and efficiently distributed on the surface. However, these lubrication methods were not widely employed because of leakage, sealing problems, and unavailability of suitable lubricant baths, which can adequately hold the lubricants during the sliding process [4]. Deng, Collins [5] tested liquid lubricants for the lubrication of micromotors and stated that liquid lubricants produce over-damping and drag in micromotors supposed that liquids are inappropriate for lubrication of MEMS. However, this statement was based on a very small amount of published literature. Their test lubricants were of high viscosities (20 to 60 cS), so it is possible that over-damping can be alleviated by using low viscous lubricants. Later, Ku, Reddyhoff [6] used liquids of low viscosities

for lubrication of MEMS thrust pad bearing and achieved low coefficients of friction at high speeds [7]. Several types of coatings such as diamond-like carbon coatings [8], amorphous carbon thin-films [9], fluorinated carbon films [10], Langmuir-Blodgett films [11], self-assembled monolayers [12] are in practice to solve the micro-scaled tribological problems where liquid lubricants cannot be employed due to precision requirement of the small parts of the MEMS devices. Thus, coatings of two-dimensional (2D) materials such as graphene, molybdenum disulfide (MoS2), and h-BN are receiving widespread attention as a potential solid lubricant because of their remarkable mechanical and tribological properties [13]. Among these 2D materials, graphene is preferred in tribological applications due to its thermal stability, low friction coefficient, high wear resistance, weak van der Waals forces, and controllable thickness [14, 15]. The layered graphene structure makes it an excellent solid lubricant, which can be used in nano or microsystems with oscillating, rotating, and sliding contacts to reduce static friction, friction, and wear [16, 17]. Liang, Bu [18] deposited graphene oxide film on a silicon specimen via electrophoretic deposition (EPD) and showed that films have high stiffness, good antiwear, and antifriction qualities. Kim, Lee [19] had grown graphene films on the Cu and Ni and transferred them onto the Si substrate, and exhibited graphene films effectively reduced the adhesion and friction forces. Liu, Li [20] tested the coatings of fluorinated graphene on steel contacts, achieved low friction and wear in different environments, and shown low wear and friction results.

This research aims to develop the graphene microfilms on the silicon MEMS devices via the CVD method and investigate their tribological performances. Surface quality and morphology, and structure of microfilms were characterized via Raman spectroscopy and AFM. Different tribological tests were carried out on a microtribometer to understand the graphene films' possible lubrication mechanism. After tribological tests, the surface morphology of worn specimens was carried out by SEM. The focus is on the effect of the different numbers of graphene films on MEMS devices' friction and wear. The excellent tribological performance indicates that CVD-grown graphene microfilms can be a potential solid lubricant for MEMS devices.

2 Experimental Design

2.1 Materials and Reagents

A single crystalline polished silicon wafer of 2 inches (thickness 500 μm) was used to fabricate MEMS devices' sliding parts. Ultrapure water and deionized water were used to wash the specimens in the Ultrasonic bath. The list of reagents and their usage is shown in Table 1.

Table 1
The list of reagents and their usage

Reagent name	Usage
PMMA Solution	Transfer of graphene film on the copper
$FeCl_3$ Solution	Etching of the Copper substrate
Acetone solution	Removing of PMMA film
Deionized water	Cleaning sample

2.2 Fabrication of the silicon friction-pair:

For the development of a sliding MEMS device, a pin-on-disk friction-pair was fabricated by loading a stationary upper specimen (a cylindrical silicon pin) of 2 mm against a reciprocating lower specimen (a rectangular silicon disk) of 15⊆10 mm. Figure 1. It shows the SEM photo of the upper specimen. A safety margin of 0.5 mm wide is kept to prevent the surface pattern's structure from being damaged during laser cutting. As a result, the actual diameter of the upper specimen is 3 mm. The pin's surface pattern is 100 μm wide, the spacing of each pattern is 100 μm, and the depth is 50 μm, and it was fabricated via DRIE.

Figure 2 (a) The real-time photo of the lower specimen holder, on which silicon wafer was mounted Fig. 2 (b) shows the lower specimen rectangular silicon disk (15⊆10 mm), which was assembled on the top of the specimen holder.

2.3 Preparation of graphene-based microfilms

For the chemical vapor deposition (CVD) growth of graphene microfilms, copper (Cu) and nickel substrates are mostly preferred catalysts. Since this research aims to study the tribological properties of graphene microfilms grown by CVD on silicon, a Cu substrate has been chosen to support the film mechanically. A Cu foil was cut into the same dimensions as the silicon wafer and was cleaned in acetone and deionized water to remove the impurities. Before starting the CVD process, the substrate was annealed at 900°C, and then graphene films were developed by the CVD process details that can be seen anywhere else [21–24].

In the next step, the prepared films were transferred onto the silicon substrates by the poly (methyl methacrylate) (PMMA) method, described in the literature [25] using the following steps.

(i) For transfer, a sacrificial film of PMMA solution was sprayed on the graphene-coated Cu substrate. (ii) PMMA film was dried at 120 ℃ for 5 minutes in an oven so that PMMA film can adequately adhere to the Cu substrate. (iii) Two Petri dishes were filled with $FeCl_3$ solution; corners of the sample were held in the solution with tweezers to etch away the graphene on the edges of the Cu foil, the sample was rinsed to clean the impurities of etchants. (iv) Then, to remove the Cu foil, the sample was placed in the $FeCl_3$

solution for 2 h, and the copper substrate was removed. (v) As a result, a strip of PMMA was left behind with graphene grown by CVD on one side. (vi) The sample was taken out from the $FeCl_3$ solution, and the sample was placed in a petri dish filled with deionized water to remove the residual impurities of the $FeCl_3$ solution. (vii) Afterward, samples were removed from the deionized water and were dried at about 110 ºC for about 1 hour. (viii) For the removal of the PMMA layer, the sample was placed in the acetone solution. This process is repeated three times every time the new acetone solution was poured, and the sample was placed for 30 minutes. (ix) After that, the sample was taken out from the acetone solution, and then acetone was blown out in normal air. Then the sample was placed in an oven for about 30 minutes at 90 ℃. Figure 3 shows the real-time photos of the final products of graphene microfilm on silicon substrates.

3 Characterization And Testing

3.1 Microtribological Characterization

After preparing microfilms on silicon samples, the surface and structural evaluation of microfilms Raman spectra were acquired for the original graphene microfilms by Raman spectroscopy (JY-HR800) at an argon − iron laser wavelength of 514 nm as the excitation source. AFM was used to study the surface morphology and quality of samples at a scanning range of 2×2 μ m, and the scanning rate was 1.01 Hz. After tribological tests, the surface morphology of worn specimens was carried out by SEM to study the lubrication mechanism and antiwear performance of the graphene microfilms.

3.2 Tribological testing

A pin-on-disk microtribometer investigated the graphene microfilms' microscale tribological behavior under different tribological parameters at room temperature and in the normal ambient environment. The prepared silicon-based pin was used as a fixed upper counterpart. A graphene-coated lower specimen disk was mounted on the tribometer's reciprocating drive, which slides reciprocally at a distance of 6 mm. Before the tribological test, all the prepared samples were cleaned in an acetone solution and dried before use. Three sets of the tribological test were carried out to investigate the effect of the different number of microfilms, loads, and reciprocating speeds. After the tribological testing, specimens were taken down from the tribometer, placed in the ultrasonic cleaner for 10 mins to remove the specimens' wear impurities. Later, deionized water and 99.9% absolute were used to clean the specimen and dried it with hot air. Then, to investigate lubrication and antiwear performance of graphene microfilms, the worn samples' wear scar morphologies were characterized through SEM.

4 Results And Discussions

4.1 Characterization of Microfilms

For the microstructural evaluation of original graphene microfilms, Raman spectra were performed before the friction tests. For the original graphene microfilms, the peak appears at 1270–1450 cm^{-1}, caused by the lattice vibration leaving the center of the Brillouin region and characterizing the defects or edges of graphene samples. The D peak appears at 1270 cm-1, the G peak, caused by the in-plane vibration of the carbon atom, appears near 1580 cm-1. The 2D peak appears near to 2700 cm-1, which is the second-order Raman peak of two phonon resonance. The intensity ratio of D and G peaks (ID/IG) is typically used to estimate graphene defect sites' concentration. The ID/IG ratio of the original graphene coating is 0.8. Figure 4 shows the obtained Raman spectra of the sample with one graphene film. It can be seen from the Raman characterization results of the sample that it is consistent with the typical graphene Raman spectra, which proves that the graphene film has been successfully prepared on the surface of monocrystalline silicon, and the graphene film has no defects.

AFM was used to characterize the surface morphology and quality of graphene microfilms and bare silicon surfaces. Figure 5 shows the AFM images of the samples with and without graphene microfilms. Figure 5 (a) shows the surface morphology of the sample without graphene films. It can be seen that the surface of the sample is uneven and has roughness. However, every roughness peak's overall height distribution is relatively uniform without significant variations, showing the silicon specimen's processing quality is according to the experimental requirements. Figure 5 (b) shows the AFM images of the sample with one graphene microfilm. It is worth noting that the sample's surface quality has been significantly improved. The overall roughness is reduced, and the surface looks much smoother than the sample's surface without the graphene film. Figure 5 (c) shows the AFM images of the sample with 2 microfilms of graphene. It can be seen that the surface quality is better than both samples. Topography photographs of graphene-coated samples reveal that the graphene was reasonably smooth. However, some fine PMMA residue and pollutants were observed on the surface of graphene films. Corresponding to the silicon surface, which has higher roughness peaks, the overall surface quality significantly improved with graphene films' deposition.

4.2 Tribological Performance

For the tribological performance evaluation of graphene microfilms, three different tribological experiments were carried out under different tribological conditions such as different loads, sliding speeds, and different numbers of graphene films.

(1) Different Number of microfilms

For this tribological study, four samples were developed with 0,1,2,3 graphene microfilms, respectively. The experiment's reciprocating speed is 5 mm/s, the applied load is 10 N, and the experimental time is 10 min. The measured friction coefficients of all four samples with different microfilms are compared in Fig. 6. It can be seen that the sample with 0 films exhibits the highest friction coefficient, and the curve has high fluctuations. The high friction coefficient can be assumed: the silicon surface has high roughness, contributing to a high friction coefficient. At the same time, fluctuations in the curves are because of debris produced during the running-in process.

On the other hand, samples with the graphene films had shown a remarkable reduction in friction coefficient. They achieved friction coefficients of 0.39, 0.31, and 0.25 for each sample, respectively, which suggests that graphene is most likely the reason for the friction reduction. It is perceived that the friction coefficient was decreasing with an increase in the number of films. Because the friction coefficient of sample 4 was the lowest than all other samples, and the friction coefficient of sample 1 was the highest. This reduction is because the number of films had increased the load-bearing capacity and reduced the samples' roughness.

Our results show a trend of friction reduction with the increase in the number of films, and the friction coefficient increase with an increase in the surface's roughness. This shows that graphene films can be used to improve the friction performance of the friction-pair.

(2) Effect of Different Speeds

For this tribological testing, a sample with two graphene films was selected, installed on the tribometer, and tribological tests were carried out at different reciprocating speeds of 5, 10, 15, and 20 mm/s. Figure 7 presents the coefficients of friction at different speed conditions. The friction coefficient for a 5 mm/s friction curve starts with high values due to surface roughness. After small-time, contaminants once all roughness on the friction track were grounded, it became stable and finally reached a value of about 0.35. However, this friction coefficient is the highest among all other curves. This is concluded that this reciprocating speed was much lower than other speeds and was not enough to properly ground all the roughness in the surfaces, which leads to the higher friction coefficient.

Further, for 10 mm/s, the friction curve starts at 0.2, increases, and becomes stable at 0.3, and remained constant with no fluctuations in the curve. The friction coefficient for 15 mm/s friction curve starts at 0.25, becomes stable at the same value, and has the lowest fluctuations. Conversely, the friction coefficient for 20 mm/s friction curve starts at 0.01 and becomes stable at 0.24.

This friction reduction can be attributed to the high speed, which had a smooth surface roughness of the graphene films quickly and helped gain the lowest friction coefficient. However, at low speeds, it had taken time to smooth the graphene film's roughness and was unable to achieve sound reduction as it has gained at high speeds. Our results showed a higher friction coefficient at lower speeds and a lower friction coefficient at higher speeds.

(3) Effect of Different Applied Loads

To study the effect of different applied loads on a graphene film, testing was carried out at 10, 20, and 30 N, while other conditions were kept the same. Figure 8 shows the friction coefficient curves under different loads. It can be seen that the smaller loads of graphene films have a good reduction in friction coefficient, while at higher loads, it has a higher friction coefficient. When the load applied was 10 N, the friction coefficient remains very low and steady at about 0.3 during the reciprocating time. Higher loads of 20 N and 30 N friction coefficient were much higher, and it was about 0.35 and 0.41, respectively.

These results indicate that the graphene films had given better protection to the specimen and increased the specimen's load-bearing capacity. However, this protection seems dependent on the applied load because when a load was small, it had the lowest friction coefficient, and when the load was high, the graphene film was worn out or quickly removed out of the wear track. Its beneficial effect is lost. Films were damaged and led to a high friction coefficient.

Therefore, it is concluded that the graphene films are vulnerable to higher loads because at higher loads after initial run-in time, the protective graphene layer is perhaps removed out of the wear track. The sliding surfaces experienced more and more metal-to-metal contact and higher adhesion levels and hence achieved higher friction. The most extended durability or the graphene film's lifetime was achieved under the lowest load 10 N. However. It is stated clearly that this experiment was performed on the three-layered sample. It is maybe possible that when the sample has more films, it could show better friction of coefficient. Our results have shown a lower friction coefficient at lower applied loads and a higher friction coefficient at higher applied loads.

4.3 Wear Performance

After the tribological testing, specimens were taken down from the tribometer, placed in the ultrasonic cleaner for 10 mins to remove the samples' wear impurities. Later, deionized water and 99.9% absolute were used to clean the specimen and dried it with hot air. The surface morphology of the specimens was analyzed with SEM, and images at different magnifications were taken. Figure 9 shows the SEM images of rubbed specimens. Figure 9 (a) shows that the specimen's SEM images without graphene films can be seen.

The specimen had deep furrows and wear marks. Wear track is highlighted with a box on the image. This can be attributed to the presence of micro convex bodies and the surface roughness of the specimen. These bodies caused the peeling of material from the abrasive marks and resulted in higher and deep wear marks. Figure 9 (b). shows the SEM images of rubbed silicon devices with one graphene film. It can be seen that with the employment of graphene films, the wear conditions are improved. Wear marks are still there, but their depth and quantity are much less than the silicon sample without graphene film. This standing of wear is possibly due to the upper specimen's reciprocating during testing, carries the wear particles on the wear track, and results in the specimen's abrasion marks. This is assumed because the graphene film's employment had increased the load-bearing capacity by increasing the contact between the specimen and helped friction-pair to bear more load. As a result, abrasion marks wear conditions were reduced than the specimen's wear conditions without graphene films. Figure 9 (c). shows the SEM images of rubbed silicon devices with two graphene films. It can be observed that wear condition is improved with the fabrication of two films of graphene on the silicon because the thickness of graphene films helped friction pair to bear more load and increased its load-bearing capacity. As a result, abrasion marks and wear conditions were reduced than the specimen's wear conditions without graphene films.

Figure 9 (d). shows the SEM images of rubbed silicon devices with three graphene films. It can be observed that wear condition is improved with the fabrication of three films of graphene on the silicon

devices because the thickness of graphene films helped friction pair to bear more load and increased its load-bearing capacity. Very slight and light wear marks can be seen in the highlighted box. It is concluded that graphene films had a good load-bearing capacity and can improve the silicon devices' wear.

It is concluded that graphene has good antiwear properties; however, this wear performance is dependent on the number of films, and the roughness in the films, roughness in the films is also a cause to increase the wear. Because of that, a sample with 1 and 2 films had also experienced little wear because it is shown in the samples' AFM images; they have surface roughness. On the whole, it has been concluded that graphene films have excellent wear reduction qualities, and they can be an excellent solid lubricant for the small-scaled silicon-based devices with moving contacts.

5 Conclusions

In summary, pure graphene-based microfilms were fabricated on the Cu substrate via a CVD technique, and developed films were transferred on the silicon substrate by the PMMA transfer method. It is intended that fabricated graphene microfilms can be a potential lubricant for the lubrication of sliding silicon MEMS devices. After developing films on silicon specimens, tribological testing was carried out by a commercial microtribometer, and the surface morphology of the worn samples was characterized with SEM. Results show that the graphene-based microfilms had remarkably reduced the friction coefficient and wear. However, microfilms' tribological performance depends on the roughness and the number of microfilms on the specimen. Therefore, it can be concluded that graphene microfilms developed via the CVD method have the potential to reduce friction and prolong the wear life of silicon MEMS and can be an effective lubricant for lubricating silicon MEMS devices.

References

1. Kumar, K.M., Shanmuganathan, P.V., Sethuramiah, A. Tribology of Silicon Surfaces: A review. Materials Today: Proceedings 5:24809–24819: (2018)
2. Almuramady, N., Borodich, F.M., Goryacheva, I.G., Torskaya, E.V.: Damage of functionalized self-assembly monomolecular layers applied to silicon microgear MEMS. Tribol. Int. **129**, 202–213 (2019)
3. Asay, D.B., Dugger, M.T., Kim, S.H.: In-situ vapor-phase lubrication of MEMS. Tribol. Lett. **29**, 67–74 (2008)
4. Ashurst, W.R., Carraro, C., Maboudian, R.: Vapor phase anti-stiction coatings for MEMS. IEEE Transactions on Device Materials Reliability **3**, 173–178 (2003)
5. Deng, K., Collins, R.J., Mehregany, M., Sukenik, C.N.: Performance impact of monolayer coating of polysilicon micromotors. J. Electrochem. Soc. **142**, 1278 (1995)
6. Ku, I., Reddyhoff, T., Wayte, R., Choo, J., Holmes, A., Spikes, H.: Lubrication of microelectromechanical devices using liquids of different viscosities. Journal of tribology 134 (2012)

7. Ku, I.S.Y., Reddyhoff, T., Holmes, A.S., Spikes, H.A.: Wear of silicon surfaces in MEMS. Wear **271**, 1050–1058 (2011)
8. Liu, H., Ahmed, S.I.-U., Scherge, M.: Microtribological properties of silicon and silicon coated with diamond like carbon, octadecyltrichlorosilane and stearic acid cadmium salt films: a comparative study. Thin solid films **381**, 135–142 (2001)
9. Anders, S., Anders, A., Brown, I., Wei, B., Komvopoulos, K., Iii, A.: J., et al. Effect of vacuum arc deposition parameters on the properties of amorphous carbon thin films. Surface coatings technology **68**, 388–393 (1994)
10. Miyake, S., Kaneko, R., Kikuya, Y., Sugimoto, I.: Micro-tribological studies on fluorinated carbon films. J. Tribol. **113**, 384–389 (1991)
11. Ginnai, T., Harrington, A., Rodov, V., Matsuno, M., Saito, K.: Langmuir-Blodgett films as lubricating layers for enhancing the useful life of high density hard disks. Thin Solid Films **180**, 277–286 (1989)
12. Maboudian, R., Ashurst, W.R., Carraro, C.: Self-assembled monolayers as anti-stiction coatings for MEMS: characteristics and recent developments. Sensors Actuators A Physical **82**, 219–223 (2000)
13. Liu, Y., Shin, D.-G., Xu, S., Kim, C.-L., Kim, D.-E.: Understanding of the lubrication mechanism of reduced graphene oxide coating via dual in-situ monitoring of the chemical and topographic structural evolution. Carbon **173**, 941–952 (2021)
14. Liu, Y., Ge, X., Li, J.: Graphene lubrication. Applied Materials Today **20**, 100662 (2020)
15. Berman, D., Erdemir, A., Sumant, A.V.: Graphene: a new emerging lubricant. Mater. Today **17**, 31–42 (2014)
16. Zhu, Y., Murali, S., Cai, W., Li, X., Suk, J.W., Potts, J.R., et al.: Graphene and graphene oxide: synthesis, properties, and applications. J Advanced materials **22**, 3906–3924 (2010)
17. Bliznyuk, V.N., Everson, M.P., Tsukruk, V.V.: Nanotribological properties of organic boundary lubricants: Langmuir films versus self-assembled monolayers. J. Tribol. **120**, 489–495 (1998)
18. Liang, H., Bu, Y., Zhang, J., Cao, Z., Liang, A.: Graphene oxide film as solid lubricant. ACS applied materials interfaces **5**, 6369–6375 (2013)
19. Kim, K.-S., Lee, H.-J., Lee, C., Lee, S.-K., Jang, H., Ahn, J.-H., et al.: Chemical Vapor Deposition-Grown Graphene: The Thinnest Solid Lubricant. ACS Nano **5**, 5107–5114 (2011)
20. Liu, Y., Li, J., Chen, X., Luo, J.: Fluorinated Graphene: A Promising Macroscale Solid Lubricant under Various Environments. ACS Appl. Mater. Interfaces. **11**, 40470–40480 (2019)
21. Bae, S., Kim, H., Lee, Y., Xu, X., Park, J.S., Zheng, Y., et al.: Roll-to-roll production of 30-inch graphene films for transparent electrodes. Nature nanotechnology **5**, 574–578 (2010)
22. El-Gamal, S., Elsayed, M.: Synthesis, structural, thermal, mechanical, and nano-scale free volume properties of novel PbO/PVC/PMMA nanocomposites. Polymer **206**, 122911 (2020)
23. Kim, K.S., Zhao, Y., Jang, H., Lee, S.Y., Kim, J.M., Kim, K.S., et al.: Large-scale pattern growth of graphene films for stretchable transparent electrodes. Nature **457**, 706–710 (2009)

24. Demirbaş, T., Baykara, M.Z.: Nanoscale tribology of graphene grown by chemical vapor deposition and transferred onto silicon oxide substrates. J. Mater. Res. **31**, 1914–1923 (2016)
25. Li, X., Cai, W., An, J., Kim, S., Nah, J., Yang, D., et al.: Large-area synthesis of high-quality and uniform graphene films on copper foils. Science **324**, 1312–1314 (2009)

Figures

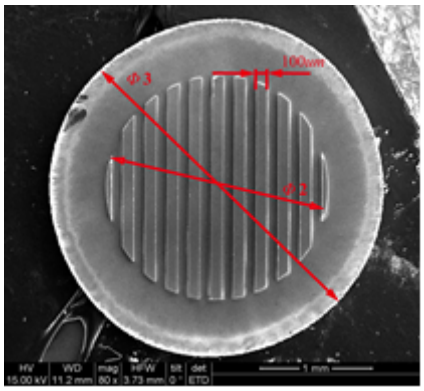

Figure 1

SEM photo of the upper specimen

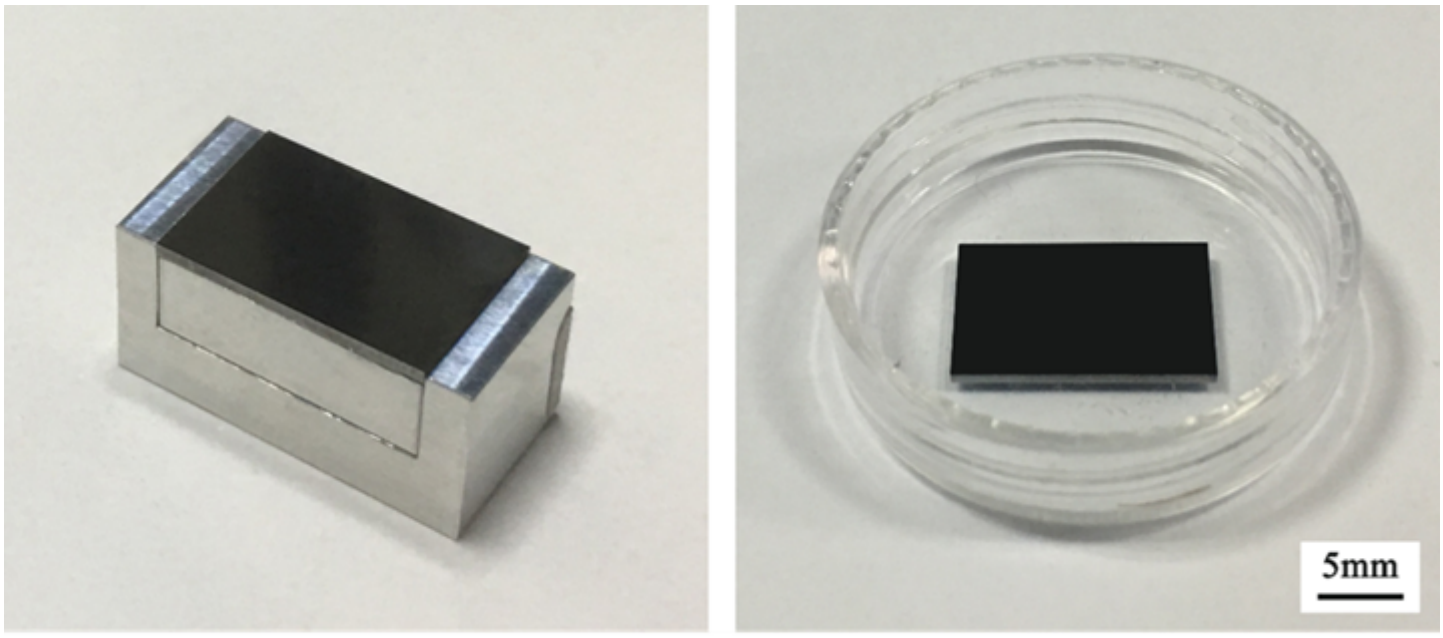

Figure 2

Real-time photos of the lower specimen holder and specimen

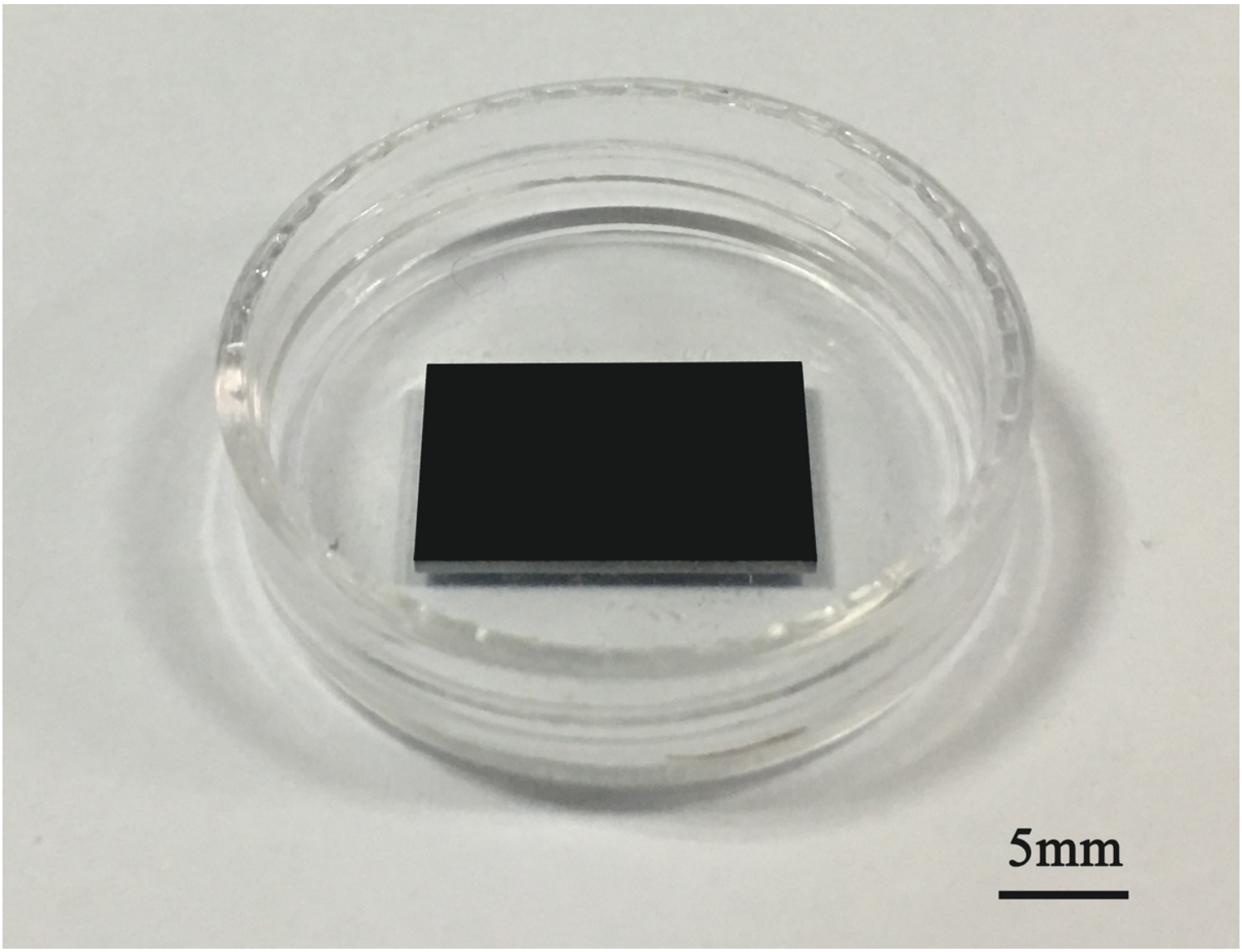

Figure 3

Real-time photos of graphene on the substrate after transfer

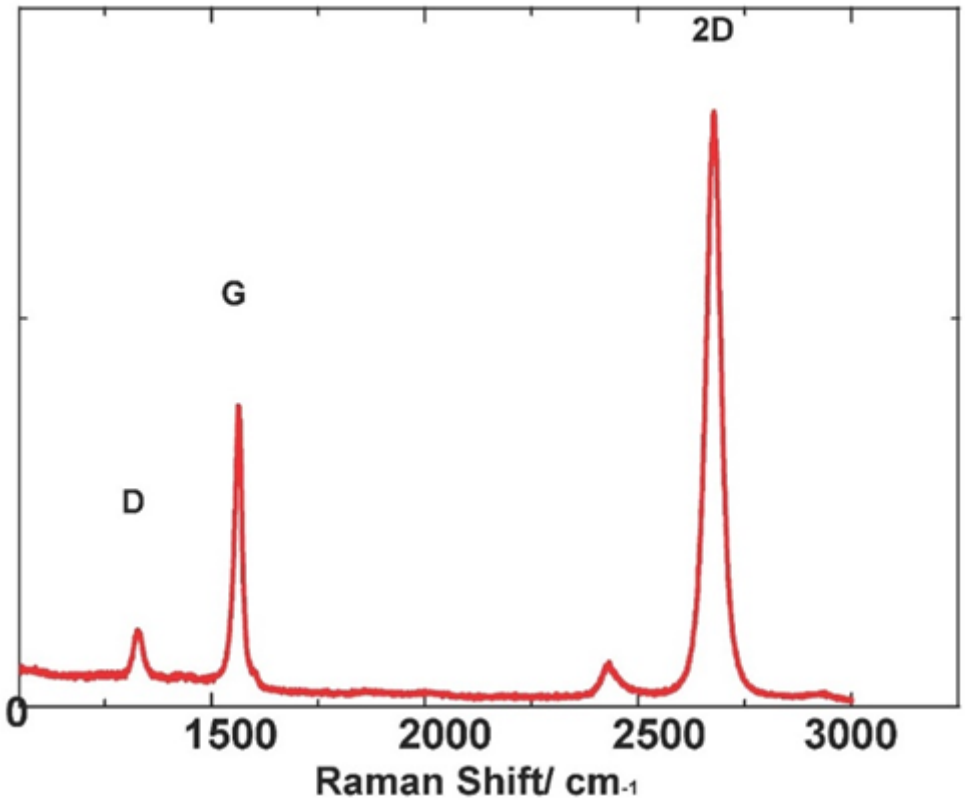

Figure 4

Typical Raman spectra of a single-layered graphene sample

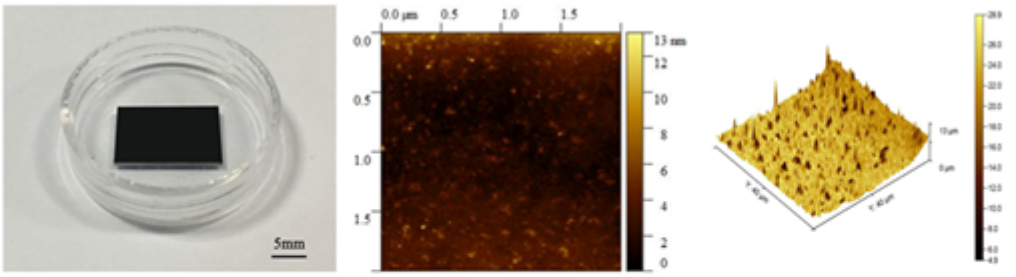

(a) AFM image of sample without graphene film

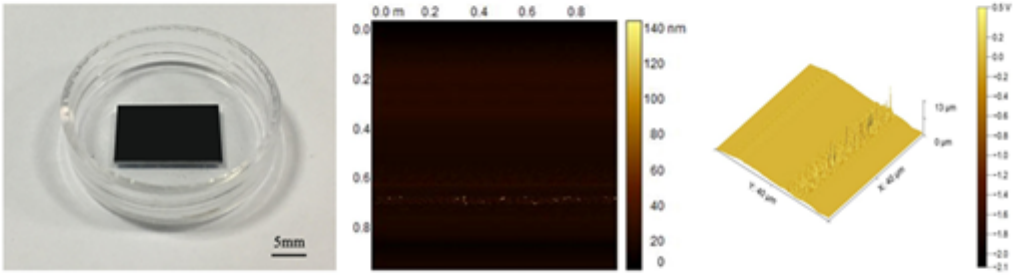

(b) AFM image of sample with one graphene film

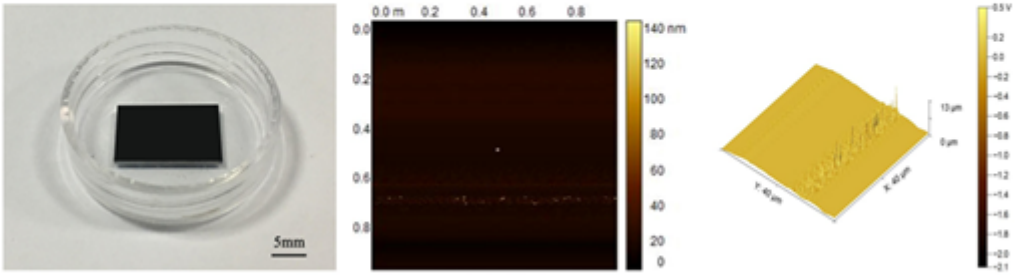

(c) AFM image of sample with graphene films

Figure 5

The AFM images of the specimens

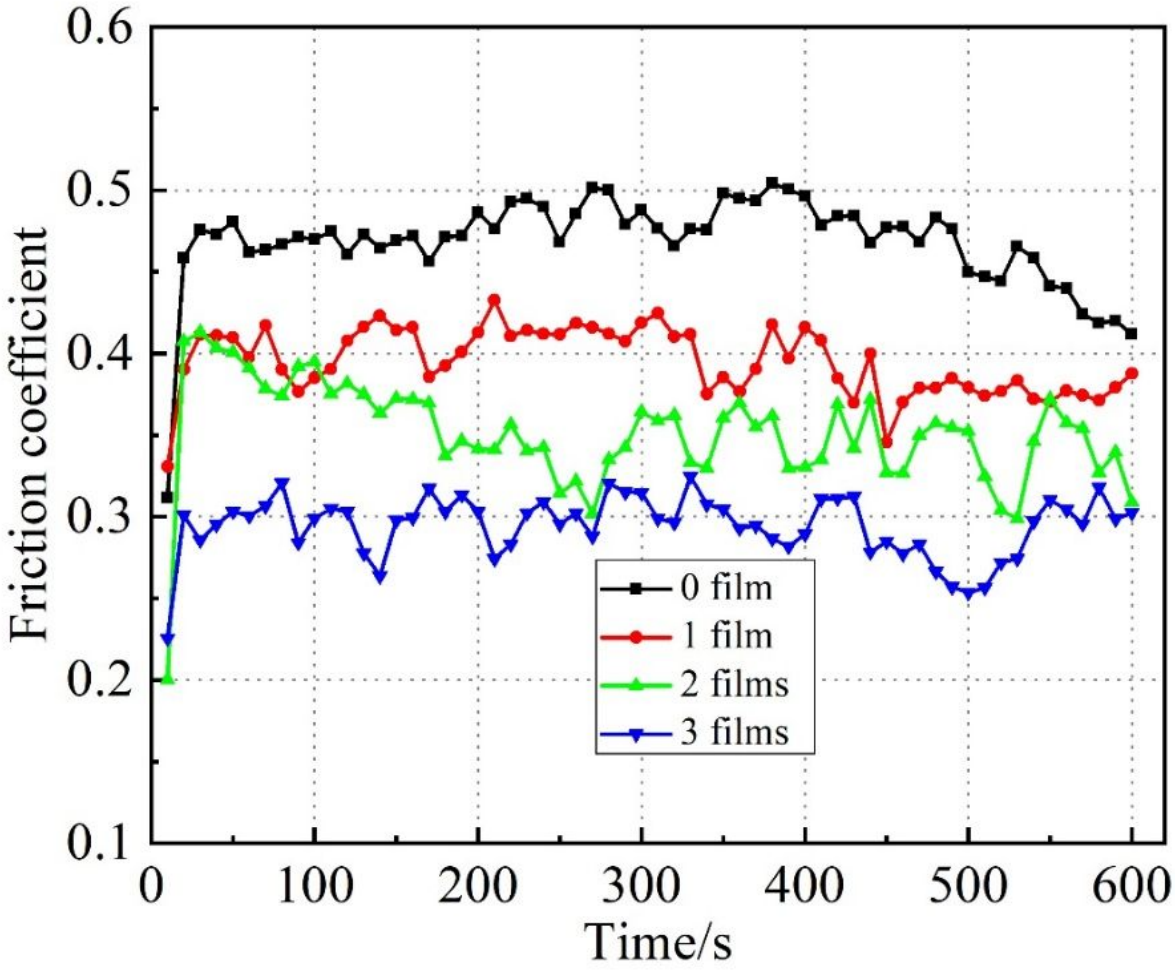

Figure 6

Friction coefficient curves at different number of graphene films

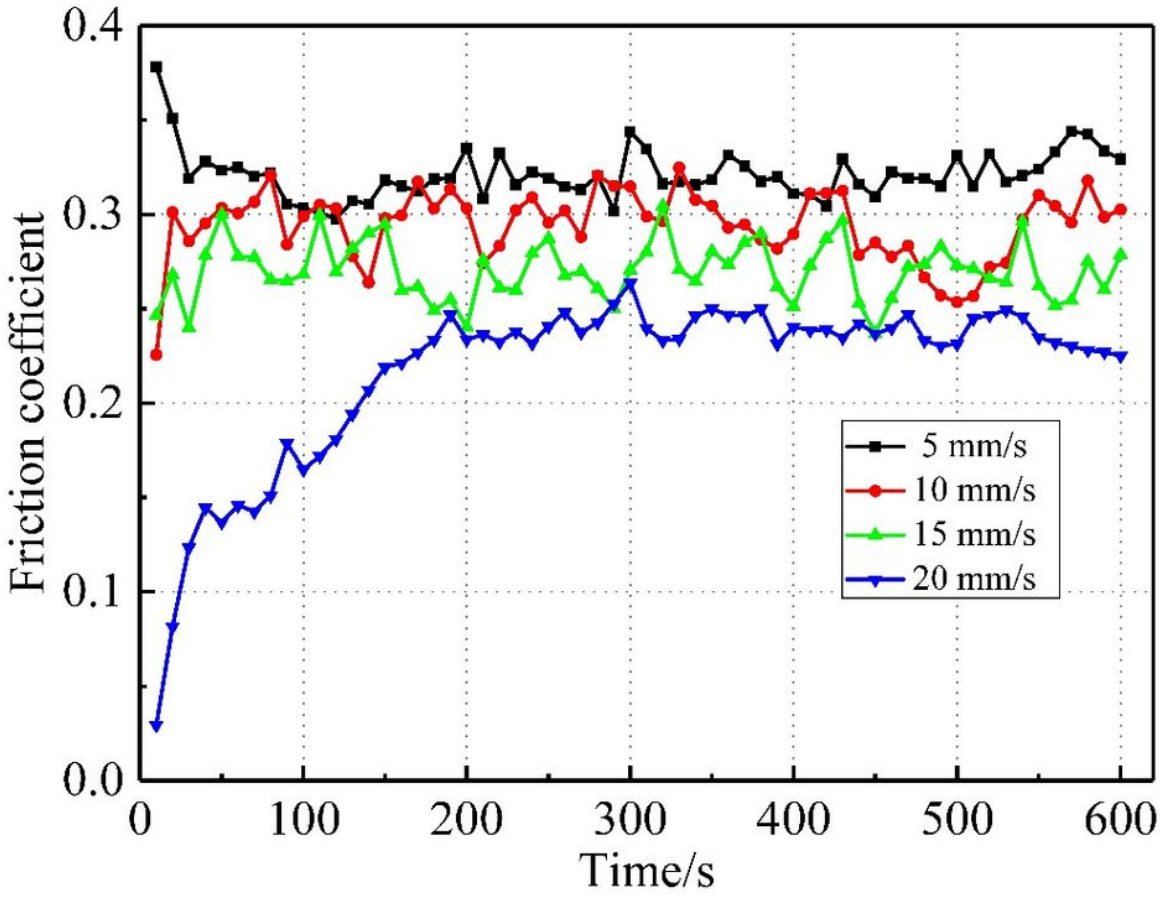

Figure 7

The friction coefficient at different reciprocating speeds

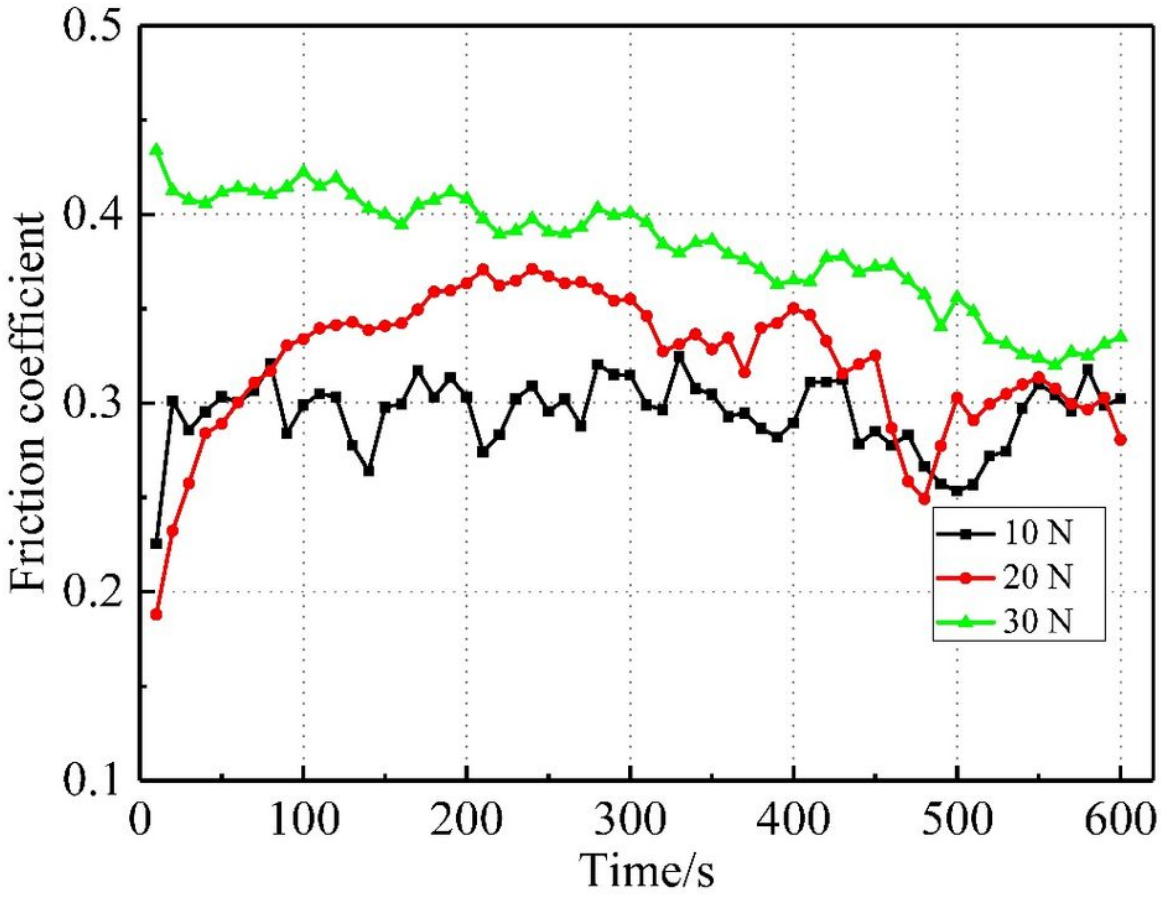

Figure 8

The friction coefficient at different applied loads

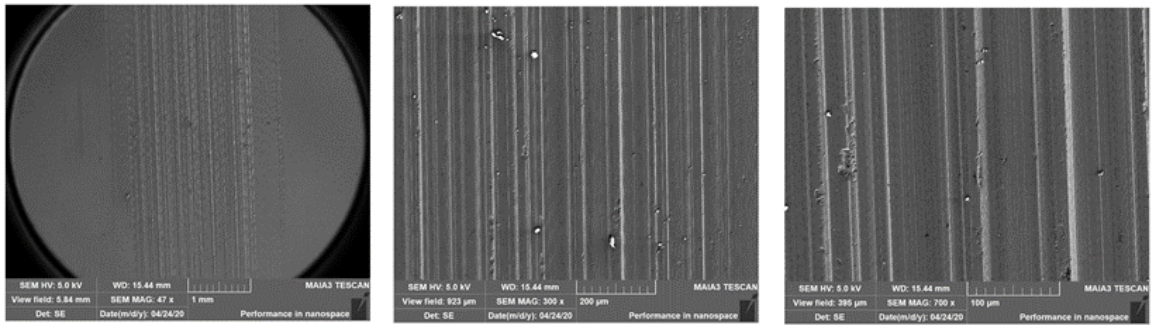

(a) SEM images of the rubbed specimen without graphene films

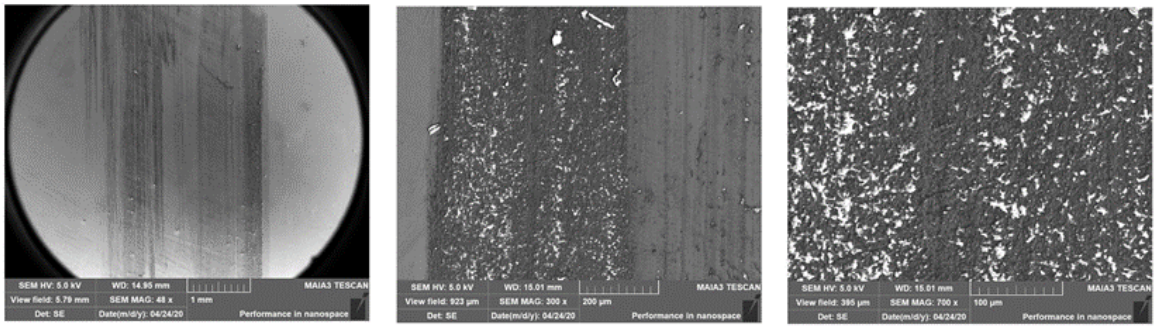

(b) SEM images of the rubbed specimen with one graphene film

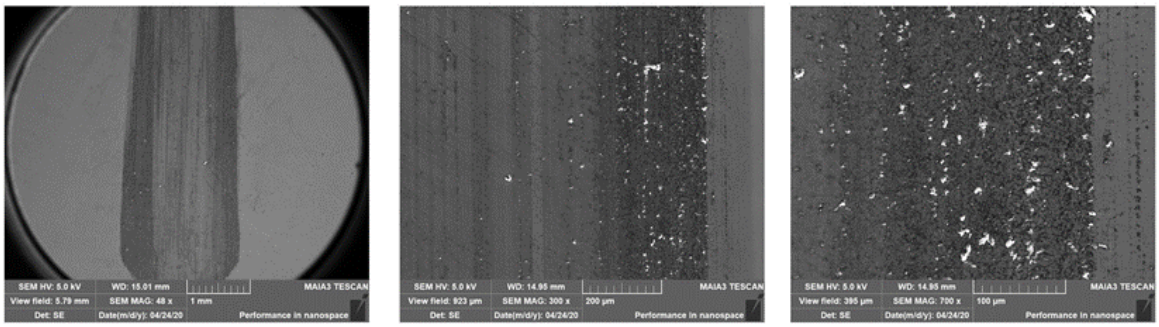

(c) SEM images of the rubbed specimen with two graphene films

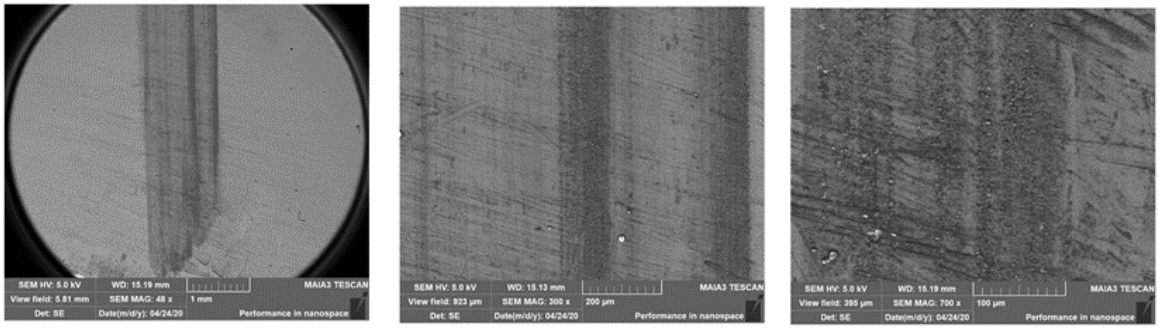

(d) SEM images of the rubbed specimen with three graphene films

Figure 9

The SEM images of rubbed surfaces